Multiphase Fluid-Loss Properties and Return Permeability of Energized Fracturing Fluids

L.H. Ribeiro, SPE, and **M.M. Sharma,** SPE, University of Texas at Austin

Summary

With the growing interest in low-permeability gas plays, foam* fracturing fluids are now well established as a viable alternative to traditional fracturing fluids. Present practices in energized fracturing treatments remain, nonetheless, rudimentary in comparison to other fracturing-fluid technologies because of our limited understanding of multiphase fluid-loss and phase behavior occurring in these complex fluids. This paper assesses the fluid-loss benefits introduced by energizing the fracturing fluid.

A new laboratory apparatus has been specifically designed and built for measuring the leakoff rates for both gas and liquid phases under dynamic fluid-loss conditions. This paper provides experimental leakoff results for linear guar gels and for N_2/guar foam-based fracturing fluids under a wide range of fracturing conditions. In particular, the effects of the rock permeability, the foam quality, and the pressure drop are investigated. Analysis of dynamic leakoff data provides an understanding of the complex mechanisms of viscous invasion and filter-cake formation occurring at the pore scale.

This study presents data supporting the superior fluid-loss behavior of foams, which exhibit minor liquid invasion and limited damage. It also shows direct measurements of the ability of the gas component to leakoff into the invaded zone, thereby increasing the gas saturation around the fracture and enhancing the gas productivity during flowback. Our conclusions not only confirm but add to the findings of McGowen and Vitthal (1996a, b) for linear gels and the findings of Harris (1985) for nitrogen foams.

Introduction

The rate of fluid leakoff to the rock formation is one of the most critical parameters involved in fracture design. The fluid invasion directly affects the fracture geometry, the fracture-closure time, and the final proppant distribution. The fracture productivity is largely related to the amount of liquid placed around the fracture. If an operator overestimates the leakoff rate, the pumping rate may be unnecessarily high and may cause excessive pump pressures. Alternatively, an operator is likely to lower the pumping rate if he underestimates the leakoff rate. In this case, the fracturing fluid may not be able to propagate large quantities of proppant along the fracture. As the proppant accumulates and the frictional pressure drop in the fracture increases, a premature screenout is likely to occur. This results in a premature job termination with a fracture that is shorter than expected.

The petroleum literature contains numerous experimental studies on the leakoff behavior of linear gels, and the reader may refer to the summaries compiled by Penny and Conway (1989) or McGowen and Vitthal (1996a, b). However, very little few are available for multi-phase fluids. Harris conducted the only systematic, published, multiphase-leakoff study on N_2 (Harris 1985) and CO_2 foams (Harris 1987).

Despite the lack of fluid-loss data, foam-based fluids have been used successfully since the mid-1970s (Grundmann and Lord 1983). They are now routinely used in low-permeability and depleted reservoirs where the drawdown forces are not sufficient to recover any fracturing fluid that invades the formation (Wendorff and Ainley 1981). Foams are also used in water-sensitive formations where clay swelling is a significant issue (Garbis and Taylor 1986; King 1986). By using foams, operators reduce the amount of water placed in the rock formation, which in turn minimizes the contact area between water and water-sensitive material. This being said, water-based foams do not eliminate the clay-swelling problem, and oil-based fracturing fluids may be preferred in case of severe clay-swelling issues. The three most obvious advantages of foms are: (1) limiting the amount of liquid placed in the rock matrix (thereby minimizing liquid blocking), (2) improving the fluid recovery (because of the presence of free gas and soluble gas coming out of solution), and (3) minimizing the contact between water and water-sensitive clays and fines.

Literature Review

Conventional leakoff analysis (Penny and Conway 1989) involves the use of a leakoff coefficient (C_w), which represents the flow resistance associated with the complex filtration process occurring at or near the fracture face. C_w depends on both the fracturing-fluid properties and the rock properties. In traditional filtration theory, C_w is obtained experimentally from the slope of the cumulative filtrate volume vs. square root of time, as described by Eq. 1. In practice, C_w is the slope of the experimental plot of filtrate volume vs. the square root of time (m), divided by the cross-sectional area of the exposed core, as shown in Eq. 2. The filtrate volume obtained before establishment of a competent filter-cake is referred to as spurt-loss volume (V_{SL}). It is obtained as the y-intercept of the linear trend attained at later times:

$$V = V_{SL} + 2C_w\sqrt{t}. \quad \ldots\ldots\ldots\ldots\ldots\ldots\ldots\ldots (1)$$

$$C_w = 0.0164 \times {}^{m}\!/_{A_c}, \quad \ldots\ldots\ldots\ldots\ldots\ldots\ldots\ldots (2)$$

Harris (1985, 1987) measured the fluid-loss properties of N_2 and CO_2 foams. He showed that foams can break down when the rock permeability is low enough. This results in the invasion of both liquid filtrate and gas at different rates. His research advocated the use of foams because they exhibited lower leakoff and insignificant damage. The main limitation of his work was the use of an impinging fluid leakoff cell that did not allow proper circulation of the fracturing fluid near the core face.

The rheology of foams has been well studied over the past 30 years. The reader may refer to Ettinger and Radke (1992) and Kovscek and Radke (1994) for the flow of foams in a porous medium, and to the work of Reidenbach et al. (1986) for the flow of foams in a pipe. At high foam quality (gas volume fraction), the interactions between gas bubbles cause a large energy dissipation that results in a high effective viscosity (Economides and Nolte 2000). The internal phase remains stable until very high qualities are reached (approximately 95%). Then, the gas becomes the external phase, and the mixture is referred to as a mist. The foam

* In this paper, we use the terms "foam" and "energized fluid" interchangeably. Strictly speaking, they refer to both the foam regime (quality typically higher than 0.52) and the co-mingled regime (quality typically lower than 0.52).

Copyright © 2012 Society of Petroleum Engineers

This paper (SPE 139622) was accepted for presentation at the SPE Hydraulic Fracturing Technology Conference and Exhibition, The Woodlands, Texas, USA, 24–26 January 2011, and revised for publication. Original manuscript received 12 November 2010. Revised manuscript received 15 October 2011. Paper peer approved 15 January 2012.

TABLE 1—RHEOLOGY CORRELATION VALUES FOR N_2 FOAMS (REIDENBACH ET AL. 1986)

HPG Load (lb/1,000 gal)	n (–)	K (lbf-sec^n/ft^2)	C_1 (–)
0	1	0.00002	3.6
10	0.75	0.0053	2.1
20	0.607	0.00256	1.7
40	0.45	0.0152	1.2

stability is the result of the quasiequilibrium between buoyancy and inertial forces, which favors gas-bubble coalescence, and the shear force, which dynamically breaks the gas bubbles and mixes them with the internal phase. At low qualities (typically less than 50%), the interactions between bubbles are minimal, so the fluid viscosity resembles that of the base fluids. Strictly speaking, the foam regime corresponds to energized fluids with qualities between 0.55 and 0.95, and the commingled-fluid regime corresponds to qualities lower than 0.5.

Reidenbach et al. (1986) studied the rheology of foams under laminar- and turbulent-flow conditions. They described the rheology of N_2/hydroxypropyl guar (HPG) foam with a Herschel-Bulkley model that depends on foam quality, gas type, and base-fluid rheology. The Herschel-Buckley model is a nonlinear rheology model characterized by three parameters: the fluid consistency K, the flow index n, and the yield shear stress τ_0. The model relates the shear stress τ experienced by the fluid to the shear rate γ as

$$\tau = \tau_0 + K\gamma^n. \quad \ldots\ldots\ldots\ldots\ldots\ldots\ldots\ldots\ldots\ldots (3)$$

In Reidenbach's work, the foam yield shear stress is uniquely a function of the foam quality for linear-gel-based foams. The yield stress significantly increases for qualities higher than 0.6, which is to be related to the large energy dissipation associated with the bubble interactions at high foam qualities. The flow index is assumed to be equal to the flow index of the sole external liquid phase. This assumption was challenged later by Khade and Shah (2004). According to Reidenbach et al. (1986), the consistency index is a function of the foam quality and of an empirical coefficient C_1, which depends on the gel loading **(Table 1).** Their formulation is given in Eq. 4, and their experimental results are provided in **Fig. 1:**

$$\begin{cases} \tau_{foam} = 0.07\Gamma \ if \ \Gamma \le 0.6 \\ \tau_{foam} = 0.0002e^{9\Gamma} \ if \ \Gamma > 0.6 \end{cases}; \quad \ldots\ldots\ldots (4)$$
$$n_{foam} = n_0;\ K_{foam} = K_0 \exp(C_1\Gamma + 0.75\Gamma^2)$$

Although Reidenbach et al. (1986) suggested that the foam viscosity increases very steeply at a quality of 52%, this threshold value depends on the surfactants and gelling agents used. It is possible to generate higher-viscosity foams at lower qualities with a different chemistry.

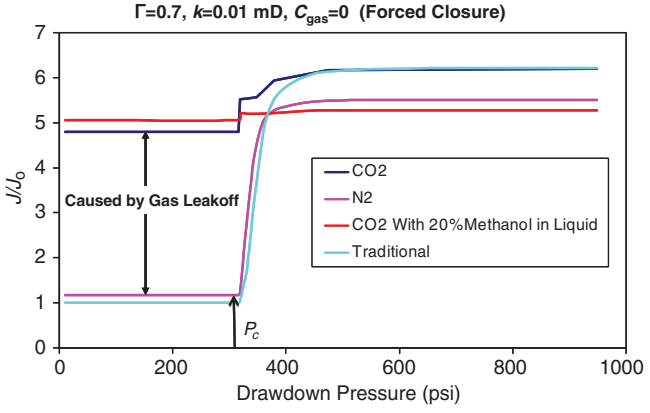

Fig. 2—Productivity index vs. drawdown pressure for several fracturing fluids (Friehauf and Sharma 2010).

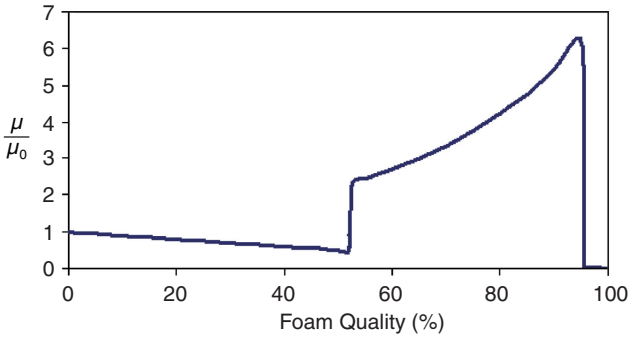

Fig. 1—Viscosity as a function of foam quality for N^2 foam with 40 lb/1,000 gal loading (Reidenbach et al. 1986).

Friehauf and Sharma (2009, 2010) have recently included the effects of multiphase leakoff into the first compositional fracturing simulator. In their model, each phase has its own leakoff properties, and the leakoff term is used in a specific mass balance for each component. Their fracturing simulator encompasses a well productivity model that is capable of evaluating the flowback performance of multiphase systems. **Fig. 2,** taken from Friehauf and Sharma (2009) shows the productivity index vs. the drawdown pressure for four fracturing treatments. The base productivity (J_0) refers to the productivity of an unfractured, undamaged well in a circular drainage area. The drawdown pressure is the difference between the reservoir pressure and the flowing bottomhole pressure. In this example, they assume that (1) the free-gas phase does not leakoff into the formation during fracturing, (2) there is no shut-in period at the end of the pumping (forced closure), and (3) the reservoir is initially at residual-water saturation. Under these conservative assumptions, the gas phase can invade the reservoir only because of solubility.

As indicated by Fig. 2, the drawdown forces were not sufficient to overcome the capillary forces for pressures lower than the reservoir capillary pressure (320 psi for a 0.01-md reservoir). As a result, the liquid phase that leaked-off re mained trapped and impeded the gas production because of relative permeability effects. For pressures higher than the reservoir capillary pressure, most of the liquid was recovered during flowback, and the treatment was beneficial. Under the given conditions of pressure and temperature, the N_2 solubility is negligible. Therefore, no gas is introduced into the porous medium, and the N_2 foam treatment does not outperform the traditional linear-gel treatment. Alternatively, carbon dioxide (CO_2) is appreciably more soluble in water under the given conditions. The release of soluble gas significantly stimulated the invaded zone. For pressures below 320 psi, the difference in performance between CO_2 and N_2 foam treatments was entirely explained by the difference in solubility between CO_2 and N_2 because we assumed that the free-gas leak off was zero in both cases. If the free-gas leak off was nonzero, these conclusions would be changed dramatically. Predicting the ability of the free gas to leakoff is thus critical when designing energized treatments.

Laboratory Equipment and Procedures

A new laboratory apparatus has been designed and built for evaluating the performance of foam fracturing fluids. The setup enables us to (1) measure the dynamic leakoff rates of both liquid and gas phases, (2) measure the foam rheology and stability over time, and (3) evaluate the rock regain permeability during flowback. The unique feature of this apparatus is the combining of multiphase fluid-loss and rheology measurements. A schematic of the system is provided in **Fig. 3.** It consists of an 850-cm^3 closed-loop system in which the fluid is prepared and circulated at fracturing conditions. The foam loop includes a foam generator, which is an in-line screen; a circulating pump (high-flow-rate gear pump);

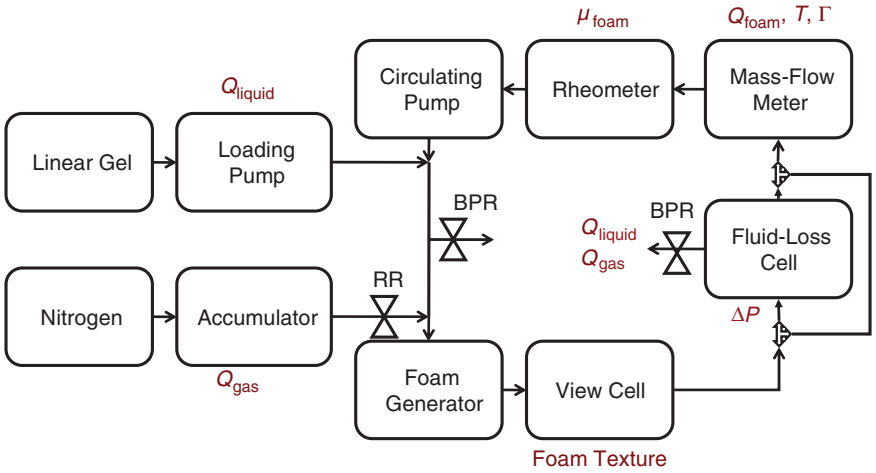

Fig. 3—Schematic of the foam-loop system, with relevant measurements shown in red.

and a mass flowmeter. Gas and liquid are loaded separately to the loop through the use of backpressure and reducing regulators (denoted by BPR and RR, respectively). The loop is connected to the fluid-loss cell, which contains the formation core.

Testing Conditions. All the experiments presented in this paper were performed for at least 90 minutes at ambient temperature (approximately 80°F) with a dynamic filtration core holder **(Fig. 4).** Unless otherwise stated, the shear rate was maintained at approximately 40 s^{-1} for the tests with linear gels and at approximately 20 s^{-1} for the tests with foams. The cores were 1 in. in diameter and 3 in. long. The pressure drop (which is the differential pressure between the core inlet and the core outlet) ranges from 450 to 1,500 psi. Fluid type and fluid composition were varied to cover a wide range of fracturing conditions. **Tables 2 and 3** detail the testing conditions for each experiment presented in this paper.

Various Berea and Nugget sandstone samples, ranging from 1 to 400 md, were used to evaluate the effects of the rock permeability. These sandstone cores were chosen because they have a high compressive strength and are quite homogeneous. Sandstone cores were preferred over limestone cores to limit flow irregularities resulting from secondary porosity. The cores were dried, vacuumed, and wrapped with Teflon™ tape and heat-shrink tubing to avoid leakage during the experiment. Cores were initially presaturated with 3% KCl brine. Before foam experiments, the cores also were flooded extensively with N_2 to reach residual-water saturation. Nevertheless, we typically did not reach the true residual-water saturation before starting the leakoff test.

The leakoff tests presented here were conducted at ambient temperature and with a backpressure set to zero (the pressure at the core outlet was atmospheric). Therefore, the foam leakoff results of this study may not be quantitatively correct under reservoir conditions. However, the underlying mechanisms of leakoff and the overall trends and conclusions should remain valid.

Fluid Preconditioning. The base fluid for both linear gels and N_2 foams was a blend of guar powder mixed with a 3 wt% KCl solution. Guar powder was mixed for an hour at a moderately high shear rate to attain proper hydration. The base-fluid rheology was measured using a traditional Fann viscometer. Readings were consistent from one batch to another. The guar solution was loaded into the foam loop at the desired pressure with the loading pump indicated in Fig. 3. The loading pump is a high-pressure syringe pump. A second pump, referred to as the circulating pump, maintained a constant flow rate at the desired pressure. This pump was a high-flow-rate gear pump capable of circulating mixtures of gas and liquid.

For foam experiments, surfactants (foamers) were added to lower the surface tension between the internal gas phase and the external liquid phase. N_2 was added to the closed loop by proper use of RRs and BPRs. The N_2 was first loaded to a 3-L accumulator pressurized at a pressure slightly above the loop pressure. A BPR was connected to the loop exit to ensure constant pressure within the loop. An RR was connected at its upstream side to the N_2 accumulator and at its downstream side to the loop. By applying a pressure at the RR slightly above the BPR pressure, the gas slowly displaced the base fluid initially present in the loop. The volume of liquid coming out of the loop was monitored to keep track of the volume of gas loaded to the loop at the pressure of interest. Once a small amount of liquid was displaced (typically 50 cm^3), the circulating pump was run at high speed to promote turbulent mixing through the foam generator (in-line screen). This

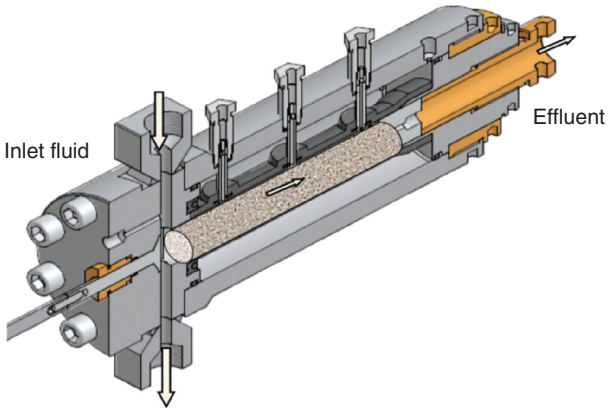

Fig. 4—Drawing of the fluid-loss cell.

TABLE 2—LIST OF EXPERIMENTS PERFORMED WITH LINEAR GELS

Fig.	ΔP (psi)	k (md)	γ (s^{-1})	Gel Loading (lbm/1,000 gal)	Cw (ft/$\sqrt{min}$)
7	550	1.5	40	30	0.0032
7	1,000	1.5	40	30	0.0033
7	2,000	1.5	40	30	0.0034
8 and 9	1,000	1.5	40	30	0.0033
8 and 9	1,000	25	40	30	0.0178
8 and 9	1,000	390	40	30	0.055
10 and 11	550	390	40	20	0.051
10 and 11	550	390	40	30	0.048
10 and 11	550	390	40	40	0.055
12	550	1.5	[7-150]	30	~0.003

TABLE 3—LIST OF EXPERIMENTS PERFORMED WITH N_2 FOAMS

Fig.	ΔP (psi)	k (md)	γ (s^{-1})	Γ	Cw_{liquid} (ft/$\sqrt{min}$)	Cw_{gas} (ft/$\sqrt{min}$)
13	450	1.5	20	0.55	0.0008	0.0005
13	950	1.5	20	0.55	0.0021	0.0020
13	1,400	1.5	20	0.55	0.0019	0.0019
14	465	390	20	0.6	0.0089	/
14	800	390	20	0.6	0.0163	/
14	1,250	390	20	0.6	0.0133	/
15	500	1.5	20	0.6	0.0008	0.0005
15	500	55	20	0.6	0.0023	0.0019
15	500	390	20	0.6	0.0089	/
16 and 17	500	55	20	0.25	0.0044	0.0005
16 and 17	500	55	20	0.5	0.0035	0.0025
16 and 17	500	55	20	0.55	0.0023	0.0019
16 and 17	500	55	20	0.65	0.0024	0.0024
18 and 19	1,000	1.5	20	0	0.0034	0
18 and 19	1,000	1.5	20	0.4	0.0023	0.0008
18 and 19	1,000	1.5	20	0.62	0.0021	0.0020
18 and 19	1,000	1.5	20	0.68	0.0017	0.0011

process was repeated step by step to safely ensure foam mixing. The foam quality increases at each step, as some gas displaces some of the liquid phase. At any time, the foam quality was calculated from the density measurements indicated by the mass flowmeter. The density of the foam was simply the weighted average of the gas and liquid densities, which were both known. The gas loading was stopped once a specific foam density was achieved. For instance, a density of 0.43 g/cm^3 indicated an N_2 foam quality of 60% at 1,000 psi.

The foam-flow rate and the pressure drop across a tubing of known dimensions were monitored over the duration of the leakoff test. The differential-pressure transducer recording the pressure drop is referred to as the rheometer in Fig. 3. The mixture was circulated at a constant shear rate until stable readings of density and viscosity were obtained over time. A high-pressure view cell was also used to provide visual inspection of the foam texture. Our rheology setup is comparable to the apparatus introduced by Hutchins and Miller (2005), who evaluated foam viscosity and stability over time with a circulating pipe as seen in Fig. 5 and Table 1 (Hutchins and Miller 2005). We adopted a very similar approach in terms of foam generation, circulation, and rheology characterization. Our apparatus allows us not only to measure the foam viscosity and the foam quality over time, but also to measure the dynamic leakoff rate simultaneously.

Fluid-Loss Cell. The fluid-loss cell is a Hassler-type core holder with a special end design allowing for dynamic testing of fluid

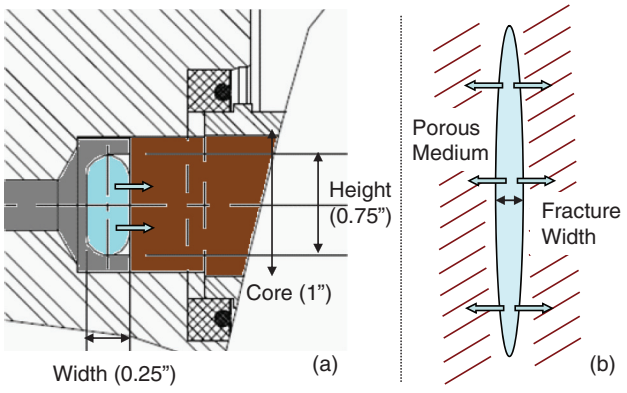

Fig. 5—(a) Drawing of the fluid-loss cell (blow-up of the special end-design) and (b) the "equivalent" flow pattern in a thin, planar, vertical fracture.

invasion into core samples, as shown in Fig. 4. With conventional core holders, the flow injection is parallel to the core. Instead, we used a core holder with a flow-through slot that allows us to flow the fracturing fluid in the direction perpendicular to the core face, the core face simply being exposed to the fracturing fluid. **Fig. 5** shows a schematic of the narrow flow conduit within the fluid-loss cell. In this figure, the end-cap is grey, the flow-through slot is blue, and the core is brown. This specific flow pattern is intended to mimic the flow path experienced by the fracturing fluid within a thin, planar fracture (Fig. 5). In Fig. 5, the major flow direction is out of the plane. This major flow direction is indicated by the thicker arrows in Fig. 4. The fluid leakoff occurs in the direction indicated by the thinner arrows in Figs. 5a and 5b.

The shear rate at the core face was estimated from the fluid-flow rate and the flow-through-slot dimensions. In this paper, the shear rate provided for the leak off experiments refers to the shear rate of the fluid in the flow-through slot (facing the core inlet). The shear rate provided in the foam rheology section refers to the shear rate within the tubing. To be consistent, the same shear rate should be experienced throughout the foam loop. This is difficult to achieve because of the numerous perturbations introduced by the valves and the in-line equipment. This being said, we chose a tubing size that gave us a shear rate similar to that in the slot. Eqs. 5 and 6 give the shear-rate expressions for the fluid flowing inside the flow-through slot and in the tubing, respectively:

$$\gamma_{slot} = \frac{6v}{w} = \frac{0.1 \times q}{w^2 \times h}. \quad \ldots\ldots\ldots\ldots\ldots\ldots\ldots\ldots\ldots (5)$$

$$\gamma_{tubing} = \frac{8v}{ID} = \frac{8 \times q}{15\pi \times ID^3}. \quad \ldots\ldots\ldots\ldots\ldots\ldots\ldots\ldots\ldots (6)$$

In Eqs. 5 and 6, q refers to the volumetric flow rate imposed by the circulating pump and measured by the mass flowmeter (in cm^3/min); v refers to the average velocity (in cm/s); w refers to the slot width (in cm); h refers to the slot height (in cm); and ID refers to the tubing internal diameter (in cm). In our setup, the slot width was 0.25 in.; the slot height was 0.75 in.; and the dimensions of the tubing were 0.5-in. outside diameter with a wall thickness of 0.035 in. For example, a flow rate of 300 cm^3/min yields a shear rate of approximately 40 s^{-1} both in the flow-through slot and in the tubing.

Dynamic Multiphase Leakoff Tests. 1-in. diameter cores were placed into an elastomeric sleeve that is subject to a radial confining stress applied with synthetic oil. Three pressure taps were placed along the core sample to monitor the extent of the fluid-invasion process over time. Dynamic leakoff tests were performed

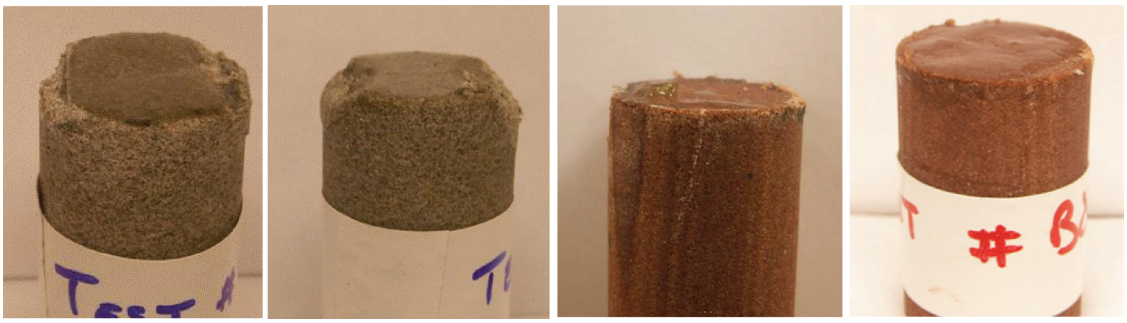

Fig. 6—External filter cakes observed after leakoff tests on Berea and Nugget sandstone samples.

for at least 90 minutes. During the leakoff test, the loading pump was operated under constant pressure to compensate for the amount of fluid leaking off. The loading pump added into the loop a volume of linear gel equal to the volume of fluid leaking off, to maintain a constant pressure in the loop during the entire leakoff test.

For most experiments, the cumulative amount of fluid leakoff was negligible compared with the volume of the foam loop (approximately 850 cm^3), and the pressure was successfully maintained constant over time. This was always the case for foam experiments. Therefore, the addition of linear gel into the loop did not significantly affect the foam quality over time. In some experiments (conducted with linear gels on high-permeability cores), the initial leakoff rate was higher than the maximum flow rate of the loading pump (28 cm^3/min). As a result, the addition of linear gel could not compensate for the amount of fluid lost through the core, and the pressure was not maintained successfully over time. An example of this is shown in Fig. 9 for the 25-md and the 400-md cores.

In this paper, the BPR was bypassed, and the pressure at the core outlet was atmospheric. The pressure drop across the core was monitored continuously with a differential-pressure transmitter connected to the core inlet and the core outlet. A high-accuracy weighing scale measured the weight of liquid effluent exiting the core over time. The gas effluent was collected at atmospheric pressure into a liquid-filled graduated cylinder. As the gas exited the core sample, it displaced the liquid out of the cylinder and the volume of gas was read directly from the graduations. The volume of N_2 was then converted back from atmospheric to testing conditions to take into account the large gas expansion.

The use of linear gels as fracturing fluids has two adverse effects, related to the liquid-filtrate invasion through the rock matrix and the deposition of polymer residues either at the core face or inside the rock matrix. Pictures of external filter cake are given in Fig. 6 for Berea (on the left) and Nugget (on the right) sandstone cores. These pictures show the establishment of a relatively thick filter cake on top of the core face exposed to the fracturing fluid. The thick, polymer-rich filter cake constitutes a low-permeability barrier that impedes the flow of gas or liquid during flowback. These pictures were taken at the end of the regain-permeability tests, which implies that the flowback of gas and brine has not entirely removed the external filter cake. The external filter-cake can constitute a long-term source of permeability damage.

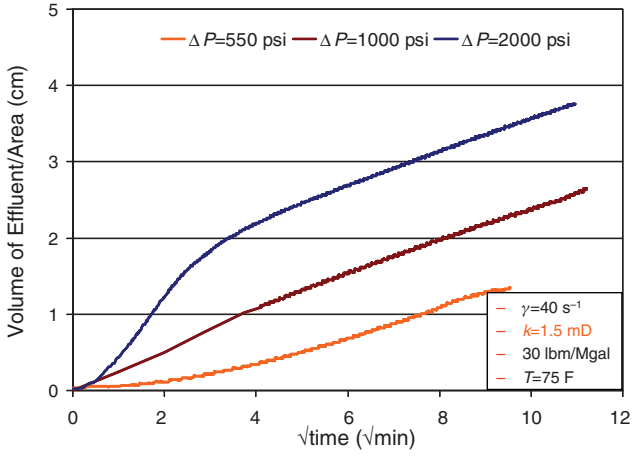

Fig. 7—Effect of pressure drop on 1.5-md cores.

Results and Discussion for Linear Gels

Approximately 30 dynamic leakoff experiments have been conducted with linear guar gels. The first goal was to assess the viability of the new experimental setup and laboratory protocols by comparing our data with what has been published in the literature. These experiments also yielded significant results that are worth discussing, either because they provide a new insight or because they confirm previous findings.

Static leak-off tests have been conducted extensively for approximately 50 years to assess the fluid-loss properties of drilling muds and fracturing fluids. However, those tests do not mimic the shear conditions experienced by the fluid during field operations. Under dynamic conditions, two competitive forces are acting on the external filter cake. The pressure gradient tends to increase the filter cake thickness whereas the shear rate applied by the circulating fluid tends to dislocate the external filter cake. When analyzing dynamic leakoff tests, one should keep in mind that the thickness and the flow resistance of the filter cake are governed by the quasiequilibrium between these two competitive effects (Jiao and Sharma 1992; Yi and Peden 1994; Navarrete et al. 1996). Nevertheless, the shear forces do not affect the internal filter cake. This pore-plugging effect gradually reduces the ability of the filtrate to flow, which complicates the analysis of dynamic leakoff data over time.

Effect of Pressure Drop. Because leakoff tests are essentially filtration tests, one can expect higher leakoff rates at larger pressure drops. The pressure drop refers here to the difference between the inlet pressure, which is the fluid pressure within the flow-through slot of the core holder, and the outlet pressure, which is the fluid pressure at the core outlet, upstream of the BPR. **Fig. 7** shows leakoff rates vs. square root of time for 30 lbm/1,000gal guar gels under filtration pressures ranging from 550 to 2,000 psi. At early times, the filtration pressure drives the fluid to flow through the core, thereby leading to large initial invasion. As the filtrate accumulates within the core sample, the resistance to flow becomes larger and the leakoff rates decrease significantly.

The wall-building leakoff coefficient is proportional to the slope of the cumulative leakoff volume vs. the square root of time after establishment of a competent filter cake. After 20 minutes, the three curves shown in Fig. 7 become linear, and their slopes are almost parallel from one test to another. Therefore, the three tests yield similar values of leakoff coefficients (0.0032 to 0.0034 ft/$\sqrt{\text{min}}$). Although the spurt loss appears to be highly affected by the filtration pressure, the leakoff coefficient does not seem to be affected by the filtration pressure, at least in our range of pressures (550 to 2,000 psi).

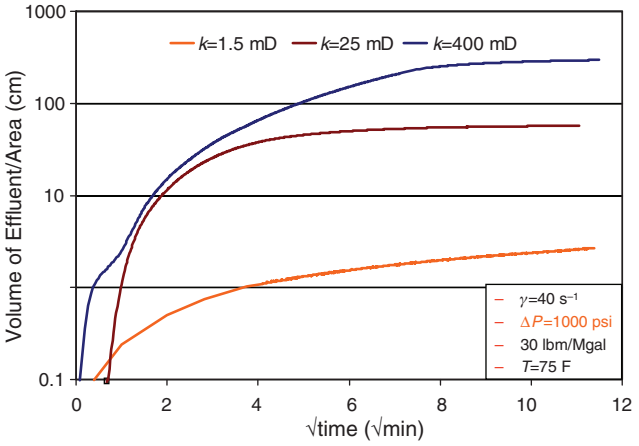

Fig. 8—Effect of rock permeability at ΔP=1,000 psi (volume of effluent).

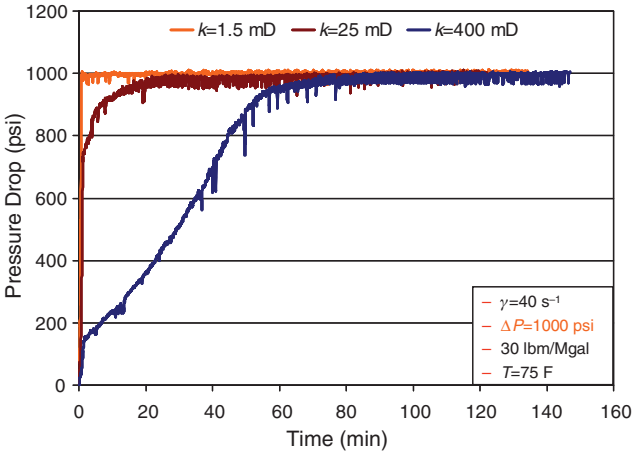

Fig. 9—Effect of rock permeability at ΔP=1,000 psi (pressure profile).

If the flow resistance (product of the permeability and the thickness) of the filter cake was independent of the applied pressure, the leakoff rate would be proportional to the filtration pressure. However, the three tests exhibit similar leakoff rates, so the flow resistance of the filter cake varies with the filtration pressure. Therefore, the filter cake is compressible. Additional tests conducted at 20 and 40 lbm/1,000 gal polymer concentration yielded very similar results; however, those results are not presented here for brevity.

Effect of Core Permeability. Figs. 8 and 9 show the cumulative leakoff volume and the pressure response of tests conducted at 1,000 psi with three core samples: Nugget sandstone (1.5 md), low-permeability Berea sandstone (25 md), and high-permeability Berea sandstone (400 md). The fracturing fluid was a 30-lbm/1,000 gal linear gel in all of these cases.

The establishment of a competent filter cake depends on the driving force applied to it. For high-permeability cores, the filtration process may not be effective for a long time, thereby yielding large spurt-loss volumes and significant invasion of the gel into the rock matrix. Fig. 9 indicates that for the high-permeability core sample, the filtration at the core face gradually becomes effective after approximately an hour. The slow increase in pressure suggests that the external filter cake is not fully established and does not seal the core face properly. This was confirmed by the presence of some polymer at the core outlet. On the contrary, effective filtration yields a transparent, polymer-free filtrate collected at the outlet. For the high-permeability-core test, the effluent was brown and opaque at early times. This indicates limited filtration at the surface and inside the core sample. For the low-permeability test, the filtration process rapidly becomes effective, as revealed by the pressure profile in Fig. 9 and the limited invasion at early times in Fig. 8.

Once a competent filter cake has been formed, the experiments show different leakoff rates for different core permeabilities. Fig. 8 exhibits leakoff coefficients of 0.0033, 0.0178, and 0.055 ft/$\sqrt{\text{min}}$ for cores of 1.5, 25, and 400 mD, respectively. As a rule of thumb, a change in two orders of magnitude in the rock permeability results in a change of one order of magnitude in the leakoff coefficient. At the pore scale, this may be explained by the extent of the pore plugging and/or polymer bridging at the core face.

As mentioned previously, the slow increase in pressure shown in Fig. 9 is undesirable and is owing to limitations in the pumping equipment. A loading pump with a higher maximum flow rate would have enabled us to compensate the large fluid losses and would have maintained a constant pressure drop across the core during the entire leakoff test.

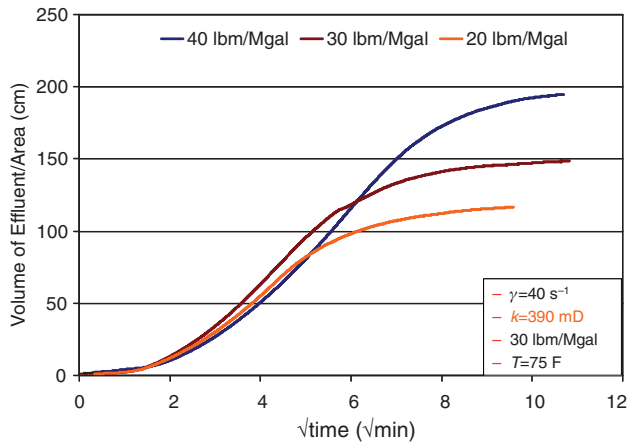

Fig. 10—Effect of gel loading on 390-md cores (volume of effluent).

Effect of Polymer Concentration. For proper fluid selection, one needs to examine numerous fluid properties, encompassing fluid ability to carry proppant, compatibility with the rock formation, and fluid-loss properties. **Figs. 10 and 11** show experiments conducted with 400-md cores at 550-psi differential pressure and with gel concentration ranging from 20 to 40 lbm/1,000 gal. Fig. 10 yields leak-off coefficients of 0.051, 0.048, and 0.055-ft/$\sqrt{\text{min}}$ for gel loading of 20, 30, and 40, lbm/1,000 gal, respectively. It implies that the fully established filter cake is not very sensitive to the gel loading under these conditions.

The time required to obtain a fully established filter cake differs in the three experiments. The location of the inflexion points on the sigmoid leakoff volume curves (Fig. 10) correlates with the decay in permeability (Fig. 11). Both indicate how the filter cake behaves over time. In Fig. 10, higher gel loadings yield larger spurt losses. This trend is consistent with other experiments conducted with core samples of 1.5 and 25 md. Increasing the gel loading increases the viscosity of the fluid and thus the internal shear force for a given shear rate. As a result, the increased shear force is more effective at dislocating the external filter cake, and it takes more time to reach the quasi equilibrium state where the shear forces and the pressure gradient applied to the filter cake balance each other.

Comparison With Published Data. The leakoff of a linear gel can depend on a multitude of parameters: e.g., core permeability, filtration pressure, imposed shear rate, fluid type, temperature, and polymer loading. This makes a direct comparison with the wealth of data in the public domain cumbersome. We compare here our leakoff data with the work published by Vitthal and McGowen

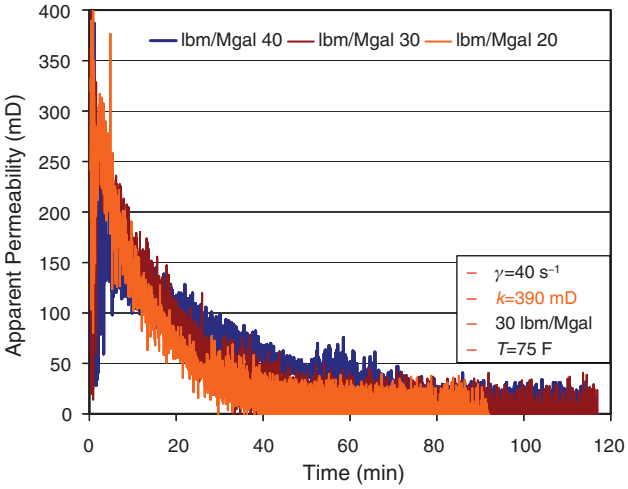

Fig. 11—Effect of gel loading on 390-md cores (permeability profile).

(1996a, b) and the work of Navarrete et al. (1995). The leakoff data and testing conditions are specified in Table 2.

The first leakoff coefficient (0.0032 ft/$\sqrt{\text{min}}$) is taken from Equation 5, page 6 (McGowen and Vitthal 1996a, b), for Ohio sandstones having permeabilities ranging from 0.3 to 1 md. It matches our leakoff data for Nugget sandstones having a permeability of 1.5 md. The second leakoff coefficient (0.027 ft/$\sqrt{\text{min}}$) is estimated from Fig. 6. (McGowen and Vitthal 1996a, b), for a 12-md Texas Cream limestone sample. The last data point (0.038 ft/$\sqrt{\text{min}}$) is taken from Table 2 (Elbel et al. 1995) for a high-permeability core (175 md). These data are consistent with our leakoff data for permeabilities ranging from 1 md to 390 md. The comparisons support the observation that the leakoff coefficient varies with the square root of the rock permeability. However, the fluid used in these papers (linear HPG) differs from the linear-guar-gel formulation we used. Our leakoff data for linear guar fluids agreed well with similar guar leakoff tests conducted by commercial laboratories. These data are not in the public domain and cannot be presented in this study. We believe that the comparisons made validate our apparatus and laboratory protocols for measuring dynamic leakoff over time.

Results and Discussion for N_2 Foams

Several papers (Harris 1985) and field observations (Grundmann and Lord 1983) have acknowledged the superior fluid-loss properties of foams. However, very limited qualitative results have supported this claim. In the field, this lack of data has contributed to occasional screenouts. Proper fracture design requires knowledge of the fluid-loss properties of the fluid to decide whether foam fracturing is more suitable than traditional fracturing. Multiphase leakoff coefficients may be used with a compositional fracturing simulator to evaluate the fracture geometry, and the return-permeability results may be incorporated in a productivity-index model to assess the potential increase in production.

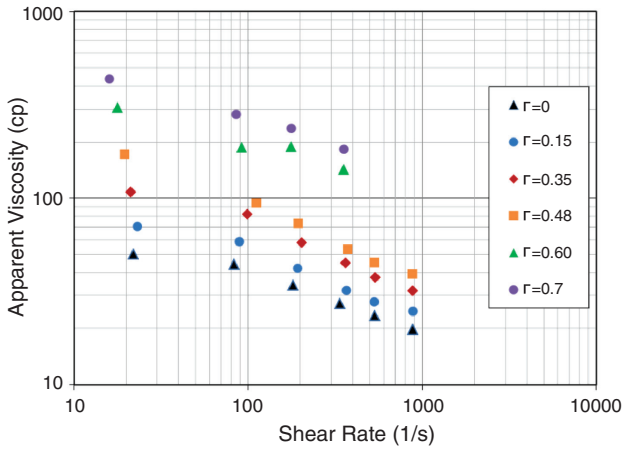

Fig. 13—Foam viscosity versus shear rate for multiple foam qualities.

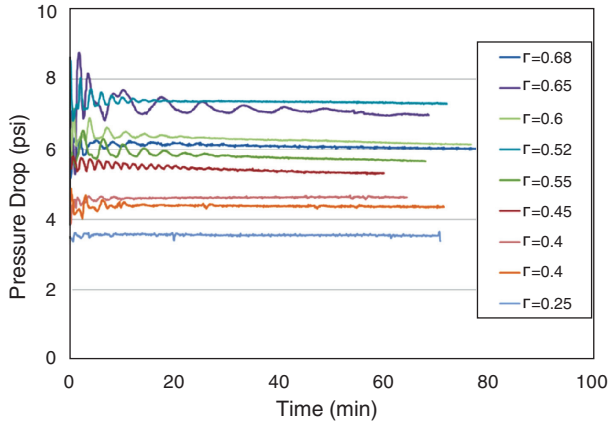

Fig. 12—Pressure drop measured in the foam loop over the duration of the leakoff test.

This paper focuses on the impact of the pressure drop, rock permeability, and foam quality on the multi-phase leakoff of N_2 foams. Other parameters are nonetheless likely to affect the foam leakoff, such as polymer loading, fluid shear rate, and reservoir pressure. For the experiments presented in this paper, the polymer loading was always 30 lbm/1,000 gal and the foam shear rate was always approximately 20 s^{-1} at the inlet.

Foam Rheology. For each leakoff test, we monitored the pressure drop within the foam loop over time. These measurements, conducted at constant shear rate, are presented in **Fig. 12.** As seen in Fig. 12, some pressure oscillations occur in the first 10 minutes. These oscillations are because of the sudden expansion of the foam caused by the opening of the valve located at the inlet of the core holder at the reference time $t = 0$. This perturbation generates some initial instability, but the oscillations disappear as the foam stabilizes. Later, the pressure drop remains constant as the foam is flowing at constant shear rate. This is a clear indication that the foam characteristics remain stable throughout the leakoff experiments. The stabilized pressure drop (and therefore the foam viscosity) increases as the foam quality increases from one test to another.

Fig. 13 shows some rheology data for N_2 foams with quality ranging from 0 to 0.7. The base gel was 30-lbm/1,000 gal linear guar; the temperature was 80°F; the loop pressure was set at 1,000 psi; and the shear rate was imposed by the circulating pump. We measured the flow rate and the pressure drop occurring along a segment of the foam loop and we converted these measurements into apparent viscosity vs. shear rate, as shown in Fig. 13. Our measurements support the fact that guar/N_2 foams are shear thinning, because the apparent viscosity decreases when the shear rate increases (regardless of the foam quality). At every shear rate, the foam viscosity increases as the quality increases. The increase in viscosity is more dramatic as the quality goes from 0.48 to 0.6. This observation is in good agreement with the widely known fact that the foam viscosity surges once the interactions between gas bubbles become dominant and cause a large energy dissipation. This surge typically occurs at a quality of approximately 0.5, as shown first by Reidenbach et al. (1986).

Our viscosity measurements are compared with the published data taken from the pioneering work of Reidenbach et al. (1986) and from Khade and Shah (2004), which constitute references widely accepted by the industry. **Fig. 14** shows the apparent viscosity measured at a stabilized shear rate of 100 s^{-1} for 30

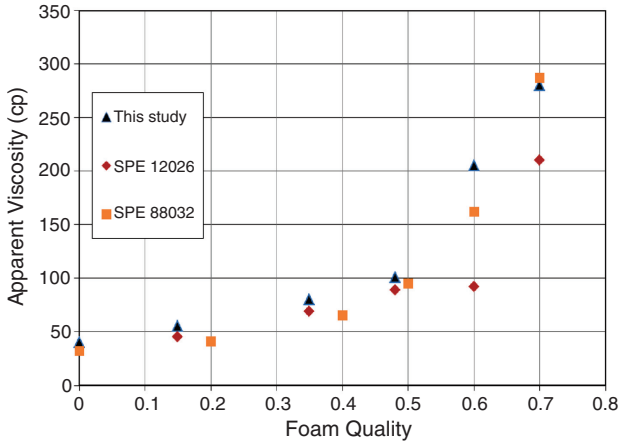

Fig. 14—Comparison of foam viscosity measurements at a shear rate of 100s−1.

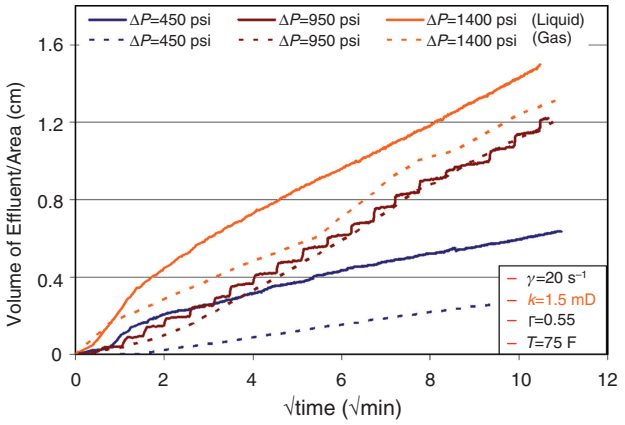

Fig. 15—Effect of pressure drop on the liquid and gas effluents for 1.5-md cores.

lbm/1,000 gal guar/N_2 foams of different qualities. The first set of data is taken from Table 1 (Reidenbach et al. 1986). The correlations presented in Table 1 (Reidenbach et al. 1986) were obtained with HPG/N_2 foam circulated in a foam loop at ambient temperature and at a pressure of 1,000 psi. On the basis of these correlations, a 30 lbm/1,000 gal HPG-N_2 foam is characterized as follows: n=0.4788, C_1=1.32, and K_f=0.0065. The apparent viscosity was then calculated from the equation presented in Table 1 (Reidenbach et al. 1986). The second set of data comes from Table 2 (Khade and Shah 2004). The rheology data correspond to a 30-lbm/1,000 gal guar/N_2 foam circulating in a loop set at a temperature of 100°F and a pressure of 1,000 psi. The apparent viscosity at 100 s^{-1} was calculated from the values of n and k provided in this table. As shown in Fig. 14, our rheology data are consistent with other published data. We have made similar comparisons under various conditions, and our rheology data agreed with the published data. This validates our apparatus and laboratory protocols for foam generation and circulation.

Effect of Pressure Drop. The foam fluid-loss behavior has been investigated on cores of 1.5, 55, and 390 md under pressures varying from 400 to 1,500 psi. **Fig. 15** shows the leakoff volume of both liquid and gas for a 0.55-quality foam exposed to a 1.5-md core. As with linear gels (Fig. 7), the filtration pressure significantly affects the initial spurt loss for both phases. Initially, the driving force applied by the pressure gradient forces the mixture to flow through the core. At later times, the filtration pressure also affects the leakoff coefficient for both phases. This behavior differs from that exhibited by linear gels. It may be explained by the highly compressible nature of the mixture, which experiences a significant volume expansion as the pressure decreases. At the pore scale, the expanding gas bubbles may push the water out, thus triggering the liquid leakoff as well. Similar fluid-loss behavior has been observed in experiments conducted on 55-md cores.

Fig. 16 shows the leakoff rates of foams exposed to 390-md Berea cores. Under these conditions, the driving force is sufficient to allow the foam mixture to flow as a whole. The foam invades the rock becasuse it can overcome the lower capillary forces exerted by larger pore throats. This behavior differs from the leakoff observed through lower-permeability cores (1.5 and 55 md). For lower-permeability rocks and for sufficiently high filtration pressures, the foam can separate into liquid and gas phases. Moreover, Fig. 16 shows that an increase in the filtration pressure increases the spurt loss but does not significantly affect the leakoff coefficient under these testing conditions. The lowest filtration pressure (465 psi) was already high enough to flow the foam through the core as a whole. We can suppose that there is a threshold pressure above which increasing the filtration pressure does not increase the leak-off rate further. Additional testing is required to investigate this behavior at high permeability.

Effect of Rock Permeability. Data were generated with 0.6-quality foams to evaluate the impact of the rock permeability on the fluid-loss behavior. **Fig. 17** shows the data collected under a 500-psi pressure drop. Similar experiments, which have been performed at 1,000 and 1,450 psi, yielded very similar results. As pointed out in the preceding subsection, foam was observed at the core outlet with the high-permeability cores. Consequently, both

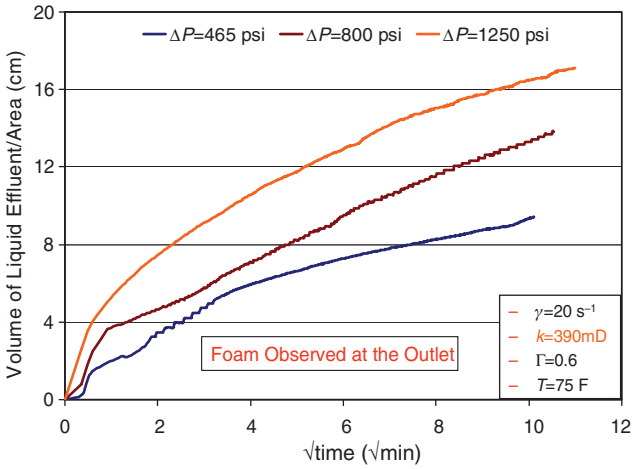

Fig. 16—Effect of pressure drop on the foam effluent for 390-md cores.

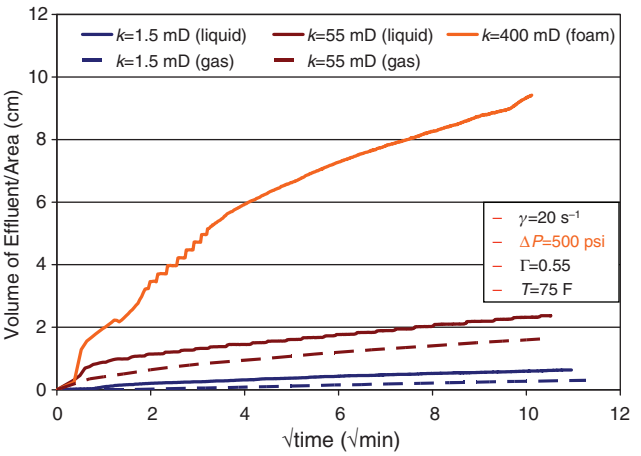

Fig. 17—Effect of rock permeability on the liquid and gas effluents for cores exposed at 500 psi.

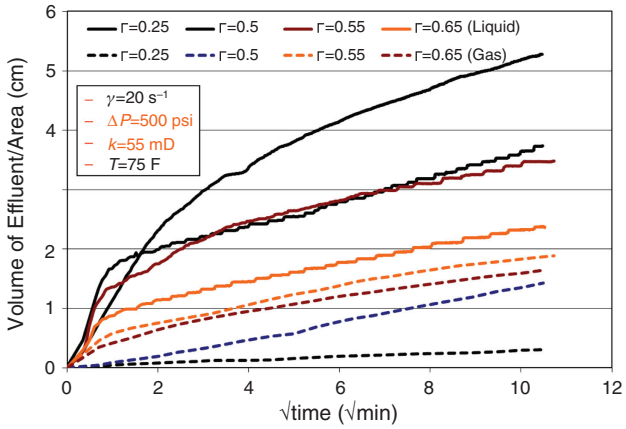

Fig. 18—Effect of foam quality on liquid/gas leakoff for 55-md cores under a 500-psi pressure drop.

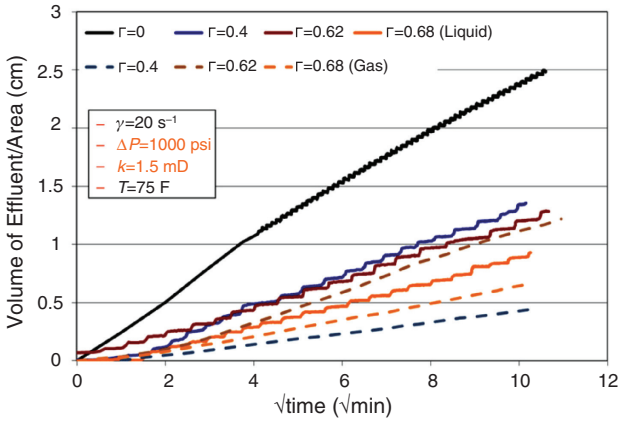

Fig. 19—Effect of foam quality on liquid/gas leakoff for 1.5-md cores under a 1000-psi pressure drop.

the spurt loss and the leakoff coefficient are significantly larger at 400 md than at lower permeabilities.

Aside from this particular behavior, the results compare well with the observations made with linear gels because the spurt loss and the leakoff coefficient of both phases are affected significantly by the rock permeability. Indeed, smaller pore throats exert higher capillary forces, thereby reducing the ability of both fluid phases to flow. This reduction in fluid leakoff is not primarily a result of the flow resistance offered by the rock; rather, it is a result of the formation of an effective filter cake on the surface of the rock. If the capillary pressure required to force the gas bubbles into the pores is larger than the filtration pressure, the leakoff of the gas phase is impeded. This dramatically reduces the invasion of the water phase for stable foams. Gas expansion inside the core can also impede the flow of water dramatically. The gas-expansion effect was more significant in our experiments, compared with the field, because no backpressure was applied.

Effect of Foam Quality. The effect of foam quality is of particular interest to us because the fluid composition is usually the only parameter the stimulation engineer can modify. **Fig. 18** shows both the liquid and gas leakoff of several N_2 foams flowing through 55-md cores under a 500-psi differential pressure. **Fig. 19** shows the liquid and gas leakoff of N_2 foams exposed to 1.5-md cores under a 1,000-psi differential pressure.

Under all conditions, foams present superior fluid-loss-control properties compared with those of linear gels, regardless of the foam quality. A comparison between Figs. 8 and 17 reveals a reduction in the liquid fluid loss by an order of magnitude at a permeability of 55 md. This reduction is less dramatic but remains significant at lower permeability (1.5 md), as illustrated in Fig. 19. The comparison between foams of different qualities show that the liquid leakoff decreases as the foam quality increases. This observation is quite intuitive, because less liquid is used at higher foam quality. Additionally, the invasion of gas into the porous medium reduces the invasion of liquid because of relative permeability effects.

Figs. 15 through 22 show the ability of the free-gas phase to leakoff under our fracturing conditions. To the best of our knowledge, this paper presents the first quantitative study of dynamic gas leakoff over time. It establishes the ability of the gas bubbles to break from the foam structure and to flow through the porous medium by a mechanism other that solubility. Figs. 18 and 19 seem to indicate that the gas leak-off increases as the foam quality increases, at least in the lower range of foam qualities. At qualities higher than approximately 60%, the gas leak-off does not seem to increase further, and it can even decrease, as shown in Figs. 18 and 19. This observation might be explained by the fundamental change occurring within the fluid at the microscopic scale. At qualities above 50% or so, the interactions between gas bubbles become preponderant, thereby increasing the internal friction and the viscosity of the foam. There is nonetheless some scatter in the data at qualities above 60%. For instance, Fig. 19 shows a surprisingly large gap between the gas leakoff of foams at qualities of 62 and 68%. In view of the discrepancies noticed in our data, we believe that it is too premature to conclude that the gas leakoff decreases with increasing inlet quality at high qualities. Additional tests at higher qualities (above 60%) and at high backpressures are needed to investigate this behavior further.

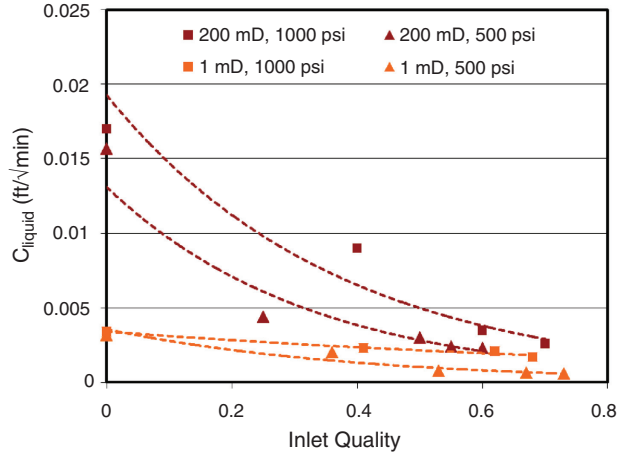

Fig. 20—Effect of foam quality on the liquid leakoff coefficient under various testing conditions.

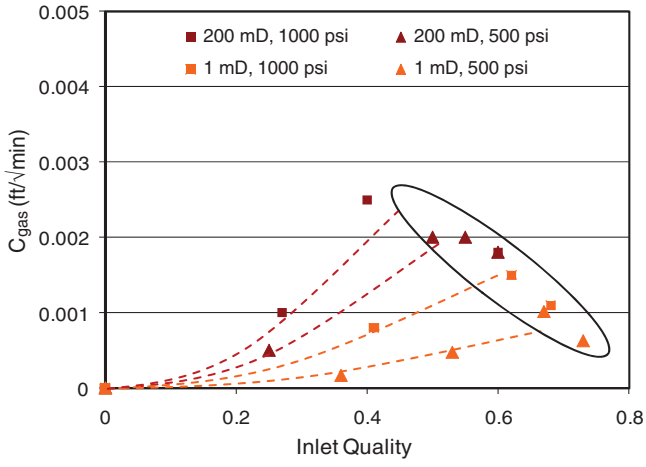

Fig. 21—Effect of foam quality on the gas leakoff coefficient under various testing conditions.

TABLE 4—COMPARISON OF FOAM LEAKOFF DATA WITH PUBLISHED DATA ON FOAMS AND WITH LINEAR-GEL LEAKOFF DATA

Nitrogen-Guar Leakoff Data (This Study)			Linear Guar Leakoff Data (This Study)		
$\Gamma = 0.6$, $T = 80°F$, $\gamma = 20\ s^{-1}$, Loading = 30 lbm/1,000 gal			$T = 80°F$, $\gamma = 40\ s^{-1}$, Loading = 30 lbm/1,000 gal		
k (md)	ΔP (psi)	C_{wtotal} (ft/$\sqrt{min}$)	k (md)	ΔP (psi)	C_{wtotal} (ft/$\sqrt{min}$)
1.5	450	0.0013	1.5	550	0.0032
1.5	950	0.0041	1.5	1,000	0.0033
55	500	0.0048	25	500	0.0167
55	950	0.0053	25	1,000	0.0178
390	465	0.0089	390	550	0.051
390	800	0.0163	390	1,000	0.055
Nitrogen-HPG Leakoff Data (Harris 1985)			Nitrogen-HPG Leakoff Data (Penny et al. 1985)		
$\Gamma = 0.75$, $T = 75°F$, $\gamma = 20s^{-1}$, Loading = 20/40 lbm/1,000 gal			$\Gamma = 0.75$, $T = 75°F$, $\gamma = 0s^{-1}$, Loading = 20 lbm/1,000 gal		
k (md)	ΔP (psi)	C_{wtotal} (ft/$\sqrt{min}$)	k (md)	ΔP (psi)	C_{wtotal} (ft/$\sqrt{min}$)
0.3	500	0.00069	0.1	1,000	0.0008
0.3	1,000	0.00134	1	1,000	0.0025
13	1,000	0.0112	10	1,000	0.0078
18.6	500	0.0108	55	1,000	0.018
17	200	0.0097	100	1,000	0.029
137	200	0.0265	390	1,000	0.048

Figures 20 and 21 show the leakoff coefficients for liquid and gas phases, respectively, under various testing conditions. These figures clearly show the effect of the foam quality on multiphase leakoff. In particular, the gas phase leaks off at a slower rate than the liquid phase, as shown in Fig. 22. The data seem to follow some general trends. This is encouraging when deriving empirical correlations for both the liquid and the gas leakoff coefficients. It is nonetheless premature to extend the general trends to lower rock permeabilities or lower pressure drop. A systematic comparison between the bubble-size distribution and the pore-size distribution would benefit our understanding of the physics of the multiphase filtration process.

Comparison With Published Data. We compared our N_2 foam leak-off data with the data published by Harris (1985) and by Penny et al. (1985). These papers are the only known references on foam leakoff. The leakoff data measured by Harris (1985) were obtained with a semistatic apparatus, which is not representative of the flow experienced in a fracture. The data from Penny et al. (1985) were obtained with a static apparatus. This is a significant difference because our study reports truly dynamic leakoff data. Also, the base fluid was a linear HPG fluid, which is different from the linear guar formulation we used. Despite these limitations, we compared these results to see whether our findings were consistent. The dynamic leakoff coefficients we are reporting here are typically lower than the values reported previously. They are nonetheless of the same order of magnitude.

The leakoff data are included in **Table 4,** which contains four sections: (1) the total (liquid+gas) leakoff coefficient of guar/N_2 foams reported in this paper, (2) the leakoff coefficient of linear gels reported in this paper, (3) the total leakoff coefficient of HPG/N_2 foams reported by Harris (1985), and (4) the total leakoff coefficient of HPG-N_2 foams reported by Penny et al. (1985). As mentioned earlier, a direct comparison with public data is cumbersome. There are very little published data for foam leakoff, and there are a multitude of parameters. The first set of data is taken from Table 1 (Harris 1985). The second set of data is taken from Fig. 10 (Penny et al. 1985). The experimental conditions are reported in Table 4 of this paper.

More significantly, we can directly compare the linear and foam leakoff data under similar experimental conditions. The use of foams greatly improves the fluid-loss-control properties as compared with linear gels. The total foam leakoff coefficient is significantly lower than the gel leakoff coefficient. This is particularly true in high-permeability formations: 0.0163 ft/$\sqrt{min}$ vs. 0.055 ft/$\sqrt{min}$ for 390-md cores, and 0.0048 ft/$\sqrt{min}$ vs. 0.0167 ft/$\sqrt{min}$ for 55- and 25-md cores, respectively. At lower permeability (1 md), the reduction in the leakoff coefficient is not as significant: 0.0013 and 0.0041 ft/$\sqrt{min}$ for the foams versus 0.0032 and 0.0033 ft/$\sqrt{min}$ for the linear gels. However, the spurt loss was significantly lower in all the cases. The ability of the foam to form a rapid-wall-building filter cake is critical in reducing the fluid loss. The leakoff-coefficient data do not capture this transient behavior, and one may also refer to spurt-loss data when evaluating the fluid-loss properties of a fluid. Under all the testing conditions reported here, energizing the fracturing fluid has reduced the total amount of fluid lost into the formation.

Return-Permeability Results

To properly capture the fluid-loss behavior of linear gels at early times, core samples were fully presaturated with brine, and the absolute permeability to brine was measured. Because no gas was introduced in the core before or during the experiment, a second brine flood was performed after the leakoff test in the direction opposite to the effluent. This second measurement gives the permeability to brine during flowback, which directly measures the fracturing-fluid-induced damage.

The ratio of the damaged to the initial permeability is given in **Fig. 23** for several linear-gel tests. Regardless of the testing conditions, the return-permeability ratio ranges from 12 to 26%, with an average value of 18%. This significant damage results from: (1) the incomplete removal of the viscous fluid that has invaded the core sample, (2) the external-filter-cake resistance, and (3) the deposition of polymer residue in the pore space. Our regain-permeability data compare well with the data published by McGowen and Vitthal (1996a, b) and Parker et al. (1994). In SPE 26559, the authors reported values of regain-permeability ranging from 5.8 to 17% on 120-md cores. The regain-permeability tests were performed after leakoff tests conducted with a 70-lbm/1,000 gal linear guar at 180°F. In Table 2 of SPE 27376, the regain permeability is approximately 7% under similar conditions. These

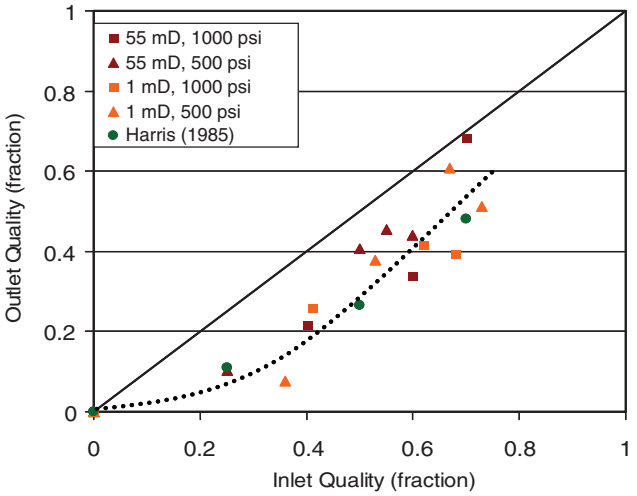

Fig. 22—Outlet composition enriched in the liquid phase as the result of filtration.

values are lower than that we measured, but the polymer loading was significantly higher in their experiments. It should also be noted that the reported regain permeability depends on the core length. Even though most of the pressure drop occurs near the core inlet (where the external filter cake is), the reported pressure drop is actually averaged along a given core length. We encourage the reader to pay attention to this detail when comparing regain-permeability data. The comparison shows that the damage associated with the use of a linear gel is quite significant, with a decrease in permeability of approximately one order of magnitude.

Foam return-permeability tests were based on a comparison between the relative permeability to N_2 before and after the leak-off test. **Fig. 24** shows return-permeability results corresponding to various nitrogen foam tests. The gas relative permeability during flowback was consistently higher than the initial gas relative permeability. This observation does not imply that the absolute permeability of the core increased. Rather, it indicates that the gas saturation increased, and so did the relative permeability to gas. Under the given fracturing conditions, the energized fluid stimulated the invaded zone. Our results show that the fracturing-induced damage is minimal and is much lower than the damage associated with linear gels. These observations are consistent with the findings of Harris, who reported regain permeabilities of approximately 90% associated with the use of N_2/HPG foams represented in Table 5 (Harris 1985). Both studies establish that the damage associated with foams is minimal.

The preceding observation is particularly important in formations in which water blocking is an issue (low- permeability formations with small drawdown). The increase in the gas saturation in the invaded zone improves the ability to flow back gas. It also enhances the cleanup of the formation. To quantify the fluid-induced damage properly, the initial permeability to gas should have been measured carefully at the true residual-water saturation.

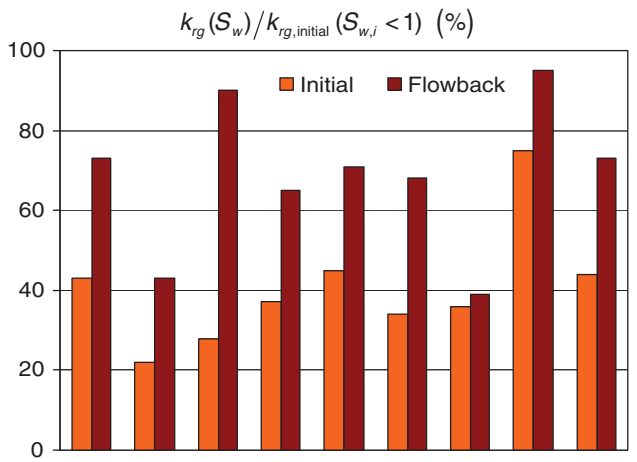

Fig. 24—Return-permeability results for N^2 foam experiments.

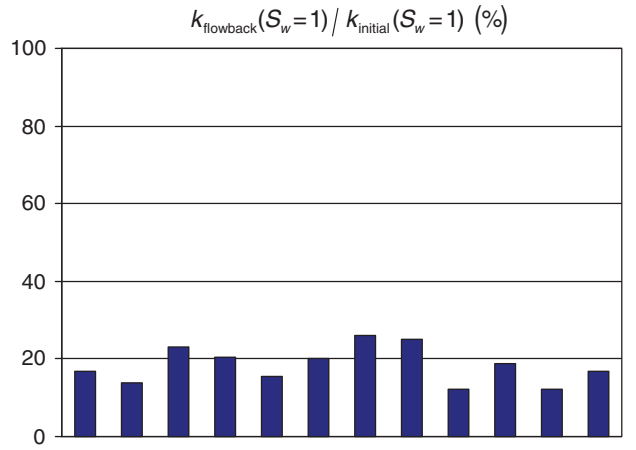

Fig. 23—Return-permeability results for linear-guar-gel experiments.

Experimental Limitations

On the basis of the analysis of the results shown in this paper, we identified two experimental limitations that should be addressed in future studies. First, the initial water saturation of the core may influence the leakoff rate at early times. Preliminary results conducted in our laboratories have revealed that an increase of the initial water saturation does not impact the liquid leakoff but does lower the initial gas-leakoff rate. This observation could explain some of the early discrepancies noticed in the gas leak-off rates presented in Figs. 18 and 19. Furthermore, the comparison of the initial and regain permeabilities is affected by the initial water saturation. This can introduce some bias when performing a round-robin fluid sensitivity study. The authors encourage the reader to carefully consider the potential changes in water saturation when analyzing leakoff and regain-permeability data.

As shown in Fig. 21, the gas leakoff was found to be somewhat erratic at high foam qualities (above 60%). It remains unclear whether this observation is to be related to the sharp increase in fluid viscosity at high foam qualities. Performing tests at high foam qualities can be a challenging task. Care should be taken when circulating high-quality foams because the foam may degrade over time. The foam integrity probably affects the multiphase leakoff. Two foams that exhibit similar quality may behave differently over time, depending on their stability. We would recommend performing an inspection of the bubble-size distribution during the leakoff test. Then, the bubble-size distribution might be related to the pore-size distribution to better understand the physics behind the filtration process occurring at the core face.

The leakoff and regain-permeability data presented here correspond to tests performed with an outlet pressure set to the atmospheric pressure. Tests performed at higher backpressures have shown some discrepancies over time. Indeed, a small pressure drop (a few psi) within the BPR results in a large volume of gas released at atmospheric conditions. This negatively affects the quality of the leak-off data over time. Highly accurate BPRs are recommended when conducting multiphase leakoff experiments.

For single-phase leakoff tests with linear gels, we found that the leakoff is not affected by the absolute pressure but only by the pressure drop across the core. However, the multiphase leakoff is suspected to be dependent on the absolute pressure, as well as on the pressure drop. In other words, a test conducted with an inlet pressure of 1,500 psi and a backpressure of 500 psi may yield results different than those of a test conducted with an inlet pressure of 1,000 psi and a backpressure set to the atmospheric pressure.

TABLE 5—EFFECT OF VARIOUS PARAMETERS ON THE FLUID-LOSS PROPERTIES

	Linear Gels		Nitrogen Foams			
	Spurt-Loss	*Cw* (liquid)	Spurt-Loss (liquid)	Spurt-Loss (gas)	*Cw* (liquid)	*Cw* (gas)
Pressure	++	=	++	++	+	+
Permeability	+++	++	+++	+++	++	++
Gel Loading	+	=	/	/	/	/
Foam Quality	N/A	NA	−	++	−	++

A sign "+/−" means that the volume of effluent increases/decreases as the parameter increases.
A sign "=" means that the effect is negligible. A sign "/" means that the effect has not been investigated yet.

Conclusions

This paper presents the first systematic experimental study of multiphase fluid loss for fracturing fluids under dynamic conditions. We introduce a new experimental apparatus with the unique capability of combining foam-rheology and dynamic-leakoff measurements over time.

Our results show good agreement with the findings of McGowen and Vitthal (1996a, b), who performed dynamic leakoff tests on linear gels, and the findings of Harris (1985), who performed semistatic leakoff tests on N_2 foams. **Table 5** compiles the sensitivity analysis for each parameter evaluated in this study. The leakoff tests presented here were conducted at ambient temperature and with a backpressure set to zero. If the foam leakoff results of this study may not be quantitatively correct under reservoir conditions, the underlying mechanisms of leakoff and the following trends and conclusions should remain valid:

1. At early times, the fluid loss of linear gels is dominated by internal invasion. Therefore, the fluid loss is highly sensitive to the core permeability and to the filtration pressure and is moderately sensitive to the gel loading.
2. At later times, the fluid loss of linear gels is dominated by the external filter cake. The leakoff coefficient appears to be sensitive to the core permeability and slightly sensitive to the shear rate. However, it is not sensitive to the filtration pressure or to the polymer loading.
3. N_2 foams containing polymers exhibit wall-building behavior and form an external filter cake.
4. N_2 foams show leakoff for both aqueous and gaseous phases at different rates. Even though the N_2 solubility is negligible, the gas phase does leak off into the invaded zone. As shown by Friehauf and Sharma (2009), this ability of the gas to leak off has a critical effect on fracture geometry and fracture design for energized fluid fracturing.
5. The use of foams greatly improves the fluid-loss-control properties of linear gels. This is particularly true in high-permeability formations where spurt loss may be considerable with linear gels.
6. At early times, both the gas and the liquid fluid losses are sensitive to the core permeability and to the filtration pressure, but to a lesser extent than with linear gels. The foam quality also impacts the fluid loss.
7. At later times, the liquid and gas leakoff coefficients depend on the core permeability, the filtration pressure, and the foam quality.
8. High-quality foams provide a slight improvement over lower-quality foams (0.3–0.5) because they further reduce the liquid leakoff. However, it is still unclear whether the gas leakoff is reduced at high foam quality.
9. In terms of fracture-induced damage, foams greatly outperform linear gels. First, foams show limited invasion of the damaging liquid phase. Second, the gas component leaking off into the invaded zone increases the gas saturation around the fracture, thereby enhancing the ability of the gas to flow back.

Nomenclature

A_c = core cross-sectional area, L^2, cm^2
C_1 = empirical correlation factor from Reidenbach et al. (1986)
C_w = wall-building leakoff coefficient, $L/\sqrt{T}$, $ft/\sqrt{min}$
k = rock permeability, L^2, md
K_0 = Herschel-Bulkley consistency index of base-fluid, NT^n/L^2, $lbf\text{-}sec^n/ft^2$
K_{foam} = Herschel-Bulkley consistency index of foam, NT^n/L^2, $lbf\text{-}sec^n/ft^2$
m = slope of an experimental plot, $L^3/\sqrt{T}$, $cm^3/\sqrt{min}$
n_0 = Herschel-Bulkley flow-behavior index of base-fluid
n_{foam} = Herschel-Bulkley flow-behavior index of foam
t = time, T, min
V = volume of effluent collected at the core outlet, L^3, cm^3
V_{SL} = spurt-loss volume, L^3, cm^3
γ = shear rate, T^{-1}, s^{-1}
Γ = foam quality (gas volume fraction)
ΔP = pressure drop across the core, N/L^2, psi
μ = viscosity, NT/L^2, cp
μ_o = base viscosity, NT/L^2, cp
τ_{foam} = yield stress of foam, N/L^2, lbf/ft^2

Acknowledgments

The authors would like to acknowledge the financial support provided by the US Department of Energy and the companies sponsoring the joint-industry project on Hydraulic Fracturing and Sand Control (Anadarko, Apache, Baker Hughes, BHP Billiton, BP, ConocoPhillips, ExxonMobil, Halliburton, Linde, Pioneer Natural Resources, Praxair, Schlumberger, Shell, and Southwestern Energy) at the University of Texas at Austin.

References

Economides, M.J. and Nolte, K.G. 2000. *Reservoir Stimulation*, third edition. New York: John Wiley & Sons.

Ettinger, R.A. and Radke, C.J. 1992. The Influence of Texture on Steady Foam Flow in Berea Sandstone. *SPE Res Eng* **7** (1): 83–90. SPE-19688-PA. http://dx.doi.org/10.2118/19688-PA.

Friehauf, K.E. and Sharma, M.M. 2009. Fluid Selection for Energized Hydraulic Fractures. Paper SPE 124361 presented at the SPE Annual Technical Conference and Exhibition, New Orleans, 4–7 October. http://dx.doi.org/10.2118/124361-MS.

Friehauf, K.E., Suri, A., and Sharma, M.M. 2010. A Simple and Accurate Model for Well Productivity for Hydraulically Fractured Wells. *SPE Prod & Oper* **25** (4): 453–460. SPE-119264-PA. http://dx.doi.org/10.2118/119264-PA.

Garbis, S.J. and Taylor, J.L. III. 1986. The Utility of CO_2 as an Energizing Component for Fracturing Fluids. *SPE Prod Eng* **1** (5): 351–358. SPE-13794-PA. http://dx.doi.org/10.2118/13794-PA.

Grundmann, S.R. and Lord, D.L. 1983. Foam Stimulation. *J Pet Technol* **35** (3): 597–602. SPE-9754-PA. http://dx.doi.org/10.2118/9754-PA.

Harris, P.C. 1985. Dynamic Fluid Loss Characteristics of Foam Fracturing Fluids. *J Pet Technol* **37** (10): 1847–1852. SPE-11065-PA. http://dx.doi.org/10.2118/11065-PA.

Harris, P.C. 1987. Dynamic Fluid-Loss Characteristics of CO2-Foam Fracturing Fluids. *SPE Prod Eng* **2** (2): 89–94. SPE-13180-PA. http://dx.doi.org/10.2118/13180-PA.

Jiao, D. and Sharma, M.M. 1992. Formation damage due to static and dynamic filtration of water-based muds. Paper SPE 23823 presented at

the SPE Formation Damage Control Symposium, Lafayette, Louisiana, USA, 26–27 February. http://dx.doi.org/10.2118/23823-MS.

Khade, S.D. and Shah, S.N. 2004. New Rheological Correlations for Guar Foam Fluids. *SPE Prod & Fac* **19** (2): 77–85. SPE-88032-PA. http://dx.doi.org/10.2118/88032-PA.

King, G.E. 1986. Foam and Nitrified Fluid Treatments-Stimulation Techniques and More. Paper SPE 14477 based on a speech presented as a Distinguished Lecture during the 1985–1986 season.

Kovscek, A.R. and Radke, C.J. 1994. Fundamentals of Foam Transport in Porous Media. In *Foams: Fundamentals and Applications in the Petroleum Industry*, ed. L.L. Schramm, No. 242, 115–163. Washington, DC: Advances in Chemistry Series, American Chemical Society.

McGowen, J.M. and Vitthal, S. 1996a. Fracturing-Fluid Leakoff Under Dynamic Conditions Part 1: Development of a Realistic Laboratory Testing Procedure. Paper SPE 36492 presented at the SPE Annual Technical Conference and Exhibition, Denver, 6–9 October. http://dx.doi.org/10.2118/36492-MS.

McGowen, J.M. and Vitthal, S. 1996b. Fracturing Fluid Leakoff Under Dynamic Conditions Part 2: Effect of Shear Rate, Permeability, and Pressure. Paper SPE 36493 presented at the SPE Annual Technical Conference and Exhibition, Denver, 6–9 October. http://dx.doi.org/10.2118/36493-MS.

Navarrete, R.C., Cawiezel, K.E., and Constien, V.G. 1996. Dynamic Fluid Loss in Hydraulic Fracturing Under Realistic Shear Conditions in High-Permeability Rocks. *SPE Prod & Fac* **11** (3): 138–143. SPE-28529-PA. http://dx.doi.org/10.2118/28529-PA.

Parker, M.A. et al. 1994. Hydraulic Fracturing of High-Permeability Formations To Overcome Damage. Paper SPE 27378 presented at the SPE Formation Damage Control Symposium, Lafayette, Louisiana, USA, 7–10 February. http://dx.doi.org/10.2118/27378-MS.

Penny, G.S., Conway, M.W, and Lee, W. 1985. Control and Modeling of Fluid Leakoff During Hydraulic Fracturing. *J Pet Technol* **37** (6): 1071–1081. http://dx.doi.org/10.2118/12486-PA.

Penny, G.S. and Conway, M.W. 1989. Fluid Leakoff. In *Recent Advances in Hydraulic Fracturing*, ed. J.L. Gidley, S.A. Holditch, D.E. Nierode, and R.W. Veatch Jr., Vol. 12, 147–176. Richardson, Texas: Henry L. Doherty Monograph Series, SPE.

Reidenbach, V.G., Harris, P.C., Lee, Y.N., and Lord, D.L. 1986. Rheological study of foam fracturing fluids using nitrogen and carbon dioxide. *SPE Prod Eng* **1** (1): 31–41. SPE-12026-PA. http://dx.doi.org/10.2118/12026-PA.

Wendorff, C.L. and Ainley, B.R. 1981. Massive Hydraulic Fracturing of High-Temperature Wells with Stable Frac Foams. Paper SPE 10257 presented at the SPE Annual Technical Conference and Exhibition, San Antonio, Texas, USA, 4–7 October. http://dx.doi.org/10.2118/10257-MS.

Yi, T. and Peden, J.M. 1994. A Comprehensive Model of Fluid Loss in Hydraulic Fracturing. *SPE Prod & Oper* **9** (4): 267–272. SPE-25493-PA. http://dx.doi.org/10.2118/25493-PA.

Lionel H. Ribeiro is a PhD candidate in the Department of Petroleum and Geosystems Engineering at the University of Texas at Austin. His current research is focused on the modeling of energized fracturing treatments with the development of the first 3D compositional fracturing simulator. Ribeiro holds a diplôme d'Ingénieur Civil des Mines degree from l'Ecole des Mines de Nancy in France and an MS degree in petroleum engineering from the University of Texas at Austin.

Mukul M. Sharma is professor and holder of the "Tex" Moncrief Chair in the Department of Petroleum and Geosystems Engineering at the University of Texas at Austin, where he has been for 26 years. He served as Chair of the department from 2001 to 2005. His current research interests include improved oil recovery, injection-water management, hydraulic fracturing, formation damage, and petrophysics. He has published more than 200 journal articles and conference proceedings and has nine patents. Sharma holds a Bachelor of Technology degree in chemical engineering from the Indian Institute of Technology, and MS and PhD degrees in chemical and petroleum engineering from the University of Southern California. Among his many SPE awards, Sharma is the recipient of the 2009 Lucas Gold Medal, the 2004 SPE Faculty Distinguished Achievement Award, the 2002 Lester C. Uren Award, and the 1998 SPE Formation Evaluation Award. He served as an SPE Distinguished Lecturer in 2002, has served on the editorial boards of many journals, and taught and consulted for the industry worldwide.